

## Spallation Ultracold Neutron Source of Superfluid Helium below 1 K

Yasuhiro Masuda,<sup>1</sup> Kichiji Hatanaka,<sup>2</sup> Sun-Chan Jeong,<sup>1</sup> Shinsuke Kawasaki,<sup>1</sup> Ryohei Matsumiya,<sup>2</sup>  
Kensaku Matsuta,<sup>3</sup> Mototsugu Mihara,<sup>3</sup> and Yutaka Watanabe<sup>1</sup>

<sup>1</sup>High Energy Accelerator Research Organization, 1-1 Oho, Tsukuba, Ibaraki 305-0801, Japan

<sup>2</sup>RCNP, Osaka University, 10-1 Mihogaoka, Ibaraki, Osaka 567-0047, Japan

<sup>3</sup>Graduate School of Science, Osaka University, 1-1 Machikaneyama, Toyonaka, Osaka 560-0043, Japan

(Received 27 July 2011; revised manuscript received 27 December 2011; published 30 March 2012)

For the production of high-density ultracold neutrons (UCNs), we placed 0.8 K superfluid helium in a cold neutron moderator. We resolved previous heat-load problems in the spallation neutron source that were particularly serious below 1 K. With a proton-beam power of  $400 \text{ MeV} \times 1 \mu\text{A}$ , a UCN production rate of  $4 \text{ UCN cm}^{-3} \text{ s}^{-1}$  at the maximum UCN energy of  $E_c = 210 \text{ neV}$  and a storage lifetime of 81 s were obtained. A cryogenic test showed that the production rate can be increased by a factor of 10 with the same storage lifetime by increasing the proton-beam power as well as  $^3\text{He}$  pumping speed.

DOI: 10.1103/PhysRevLett.108.134801

PACS numbers: 29.25.Dz, 28.20.-v, 67.25.-k

Cohen and Feynman proposed to use neutron inelastic scattering to demonstrate the existence of elementary excitations in superfluid helium (He-II) [1], predicted earlier by Landau [2]. In 1977, Golub and Pendlebury proposed to use these elementary excitations for the production of ultracold neutrons (UCNs) [3]. They predicted a very large UCN density in He-II, placed in a cold neutron source, at temperatures below 1 K. The phase-space density of the neutron is greatly enhanced upon phonon excitation, because a large phonon phase-space can be used. Therefore, it is free from the limitations of Liouville's theorem. Because UCNs are completely reflected from the surface of appropriate materials, they can be confined in a bottle. High-density UCNs are required in a number of experiments, involving, e.g., the measurements of the neutron electric dipole moment,  $\beta$  decay, and gravity. Since the proposal of Golub and Pendlebury, many UCN production studies have been carried out where He-II was placed in cold neutron beams at nuclear reactors [4–8]. The UCN production rates observed were consistent with the prediction [9], but small, because the guides subtended very small solid angles to the cold neutron sources.

Phonon excitation in solid deuterium was also used in the production of UCNs [10,11], because solid deuterium has a higher production rate  $P$ . The storage lifetime  $\tau_s$  in He-II is larger, because  $^4\text{He}$  nuclei do not absorb neutrons. The UCN density is represented by the product of  $P$  and  $\tau_s$ . The value of  $\tau_s$  is limited by phonon upscattering, which has, e.g., a time constant of  $\tau_{\text{ph}} = 36 \text{ s}$  at 1.2 K and 600 s at 0.8 K [4]. The production rate, i.e., the product of the cold neutron flux and the phonon excitation cross section, is limited by neutron-capture  $\gamma$  heating, because  $\tau_{\text{ph}}$  depends on the He-II temperature.

We have, for the first time, placed He-II with a temperature below 1 K in a dedicated cold neutron source coupled to a spallation neutron target. A higher UCN production rate is expected compared to the reactor experiments

because of the higher cold neutron flux. However, the heat load on the He-II becomes more serious, particularly at temperatures below 1 K. Additional difficulties arise from the heat load of thermal radiation and superfluid-film flow in the UCN guides needed for the transfer of the neutrons to an experimental apparatus. We have resolved these problems in a new He-II cryostat designed for temperatures below 1 K. As a result, a production rate of  $P = 4 \text{ UCN cm}^{-3} \text{ s}^{-1}$  and a storage lifetime of  $\tau_s = 81 \text{ s}$ , much longer than the value with the previous He-II cryostat for 1.2 K [12], were obtained. The proton-beam power was  $400 \text{ MeV} \times 1 \mu\text{A}$ . We have studied the thermal properties of He-II in conjunction with  $\gamma$  heating. As a result, we find that the present UCN source can provide  $P = 40 \text{ UCN cm}^{-3} \text{ s}^{-1}$  with  $\tau_s = 81 \text{ s}$  by using a proton beam with higher power and by applying  $^3\text{He}$  pumping with higher speed. Both are presently available. Thus we expect the present UCN source to have a great impact on the field of physics where high-density UCNs are required.

*Spallation UCN source.*—Our UCN source is installed at RCNP, Osaka University. Figure 1 shows the layout of the UCN source. The He-II bottle consists of an aluminum tube with a wall thickness of 2 mm, a diameter of 16 cm, and a length of 41 cm. The volume of He-II is 8 L. The inside of the bottle is coated with nickel by applying electroless plating. It is immersed in a 20 K cold neutron moderator of heavy water. The cold neutron flux was estimated by using the Monte Carlo simulation code PHITS assuming the 20 K heavy water behaves like an ideal gas [13]. The calculated flux at the resonant energy for single-phonon excitation  $E^*$  is  $d\phi(E^*)/dE^* = 9.3 \times 10^8 \text{ neutrons cm}^{-2} \text{ s}^{-1} \text{ meV}^{-1}$  for a proton-beam power of  $400 \text{ MeV} \times 1 \mu\text{A}$ . The  $\gamma$  heating in the He-II is 91 mW. The production rate for UCNs of energies lower than  $E_c = 210 \text{ neV}$ , which is limited by the Fermi potential of the nickel plating, was calculated to be  $9 \text{ UCN cm}^{-3} \text{ s}^{-1}$  for a single-phonon excitation and  $14 \text{ UCN cm}^{-3} \text{ s}^{-1}$  including

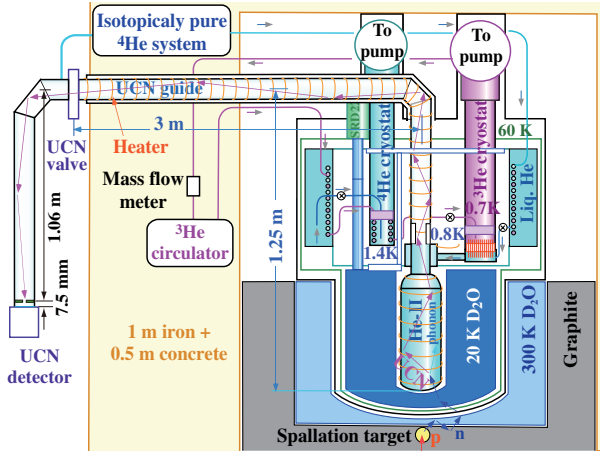


FIG. 1 (color online). He-II spallation UCN source. A He-II bottle, which is surrounded by 300 and 20 K heavy waters, is cooled by a  $^3\text{He}$  cryostat. UCNs produced by phonon excitations in the He-II are confined in a He-II bottle and UCN guides that can be closed by a UCN valve. For UCN counting, the valve is opened so that UCNs go to a UCN detector. An aperture disk is placed at the end of the guide before the detector window of aluminum.

multiphonon excitation using the formulas of Ref. [9]. However, the ideal gas assumption is not fulfilled, because deuterons and oxygen nuclei are strongly bound in the solid heavy water. Therefore, the effective masses for cold neutron scattering are larger and the neutron temperature is higher, for example, 50 K [14]. In the simulation, the neutron temperature was in equilibrium with the ideal gas of cold heavy water, and we used, therefore, a higher cold-moderator temperature. At temperatures of 50 and 80 K, the UCN production rates become 6 and 4 UCN  $\text{cm}^{-3} \text{s}^{-1}$ , respectively, including multiphonon excitations.

The He-II bottle is connected to a double-walled tube of stainless steel. The outer part is vacuum tight and connected to a liquid helium condensation reservoir through a 2.5 cm diameter stainless-steel pipe. The condensation reservoir is attached to the bottom of the  $^3\text{He}$  cryostat so that  $^4\text{He}$  gas is cooled through a heat exchanger of copper fins and then condensed to liquid helium [15]. The liquid helium enters the He-II bottle through a slit of 50  $\mu\text{m}$  width at the inner part of the double tube and then fills the bottle at the level of the upper part of the double tube. The temperature of the liquid helium is lowered to 0.8 K by pumping using a Roots blower of 2000  $\text{m}^3 \text{h}^{-1}$  circulating the  $^3\text{He}$  gas. A precooling line for the  $^3\text{He}$  gas is installed in the He-II cryostat for high-power operation. The double tube is directly connected to a vertical UCN guide without a cryogenic window. Liquid helium becomes superfluid below a temperature of 2.17 K. The inner diameter of the guide tube is 8.5 cm except for the connecting part with a diameter of 5 cm, where superfluid-film flow is suppressed because of the smaller perimeter. The vertical tube is connected to a horizontal tube of 3 m length. The total

volume of the UCN guide tubes is 22 L. The overall length of the vertical guide tube including the He-II bottle is 1.25 m. The horizontal tube is connected to a UCN valve, where experimental apparatuses can be attached. The He-II level in the 5 cm diameter connecting part is controlled in order to suppress the superfluid-film flow to the vertical tube and also to maintain good heat conduction between the He-II bottle and the  $^3\text{He}$  cryostat. A radiation shielding and a baking heater are installed at the outside of the vertical and horizontal guide tubes.

*UCN production.*—A 400 W proton beam impinged on the spallation target for a duration of 100 s. During this time, the UCN valve was closed. The UCNs accumulate in the phase-space volume homogeneously. Downstream of the UCN valve, a UCN detector (DUNia-10) was connected to the end of a UCN guide tube with a volume of 6 L. In a first test, the aperture disk shown in Fig. 1 was removed. After switching off the proton beam, the UCN valve was opened so that UCNs could drift to the detector. A very large number of UCNs were counted as shown in Fig. 2. The counts during the proton-beam impingement arise from background neutrons and  $\gamma$ 's. The fast rise of neutron counts just after the UCN valve was opened shows a UCN diffusion. The decrease in the neutron counts after the peak reflects UCNs emptying as they disappear in the detector.

Subsequently, we inserted the aperture disk in front of the UCN detector. Since the outer disk diameter was 8.5 cm, much larger than the diameter of the center hole, 1 cm, most of the UCNs are reflected by the disk. UCN loss arises from the hole, and also wall collisions and  $^3\text{He}$  absorption, in addition to the phonon upscattering and the  $\beta$  decay. The UCNs go back and forth in the UCN container between the disk and the He-II bottle through the guide tubes. During this motion, the UCNs as a whole experience an average loss rate, which is the inverse of a decay time constant. A buildup time constant of UCN production is the same as the decay time constant. We confirmed it by using a simulation [16].

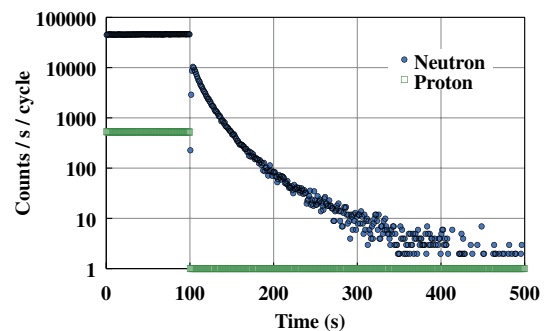


FIG. 2 (color online). UCN counts after a 100 s proton-beam pulse of 1  $\mu\text{A}$ . The squares are proton counts. The circles are UCN counts.

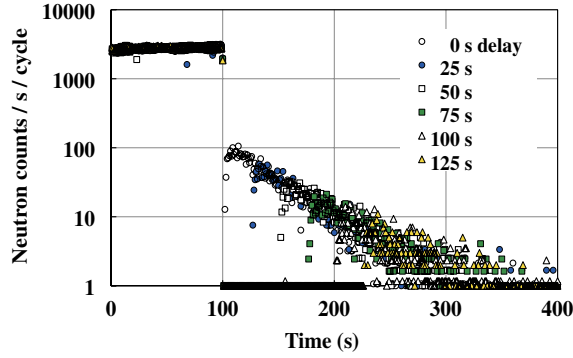


FIG. 3 (color online). Storage-lifetime measurement by opening and closing the UCN valve. The open circles, closed circles, open squares, closed squares, open triangles, and closed triangles are the UCN counts for 0, 25, 50, 75, 100, and 125 s delays in UCN valve opening, respectively. In these measurements, the aperture disk is placed in front of the UCN detector.

For the storage-lifetime measurement, a proton beam of  $0.2 \mu\text{A}$  impinging on the spallation target for a duration of 100 s. After a time delay of  $t_d$ , the UCN valve was opened and the UCN events were counted in the detector. The results are shown in Fig. 3. The decay spectra for  $t_d = 0, 25, 50, 75, 100,$  and  $125$  s are represented by a time constant as expected. These decays arise from UCN losses in the UCN container including the losses in the detector. The decrease in the sum of UCN counts after valve opening as a function of  $t_d$  is represented by a time constant of  $\tau_s = 47$  s.

We have estimated the UCN density  $\rho$  at the UCN valve by using the count rate just after valve opening, represented by  $U \cdot \rho \cdot \epsilon$ , where  $U$  is the UCN conductance, represented by  $1/U = 1/U_0 + 1/U_{90} + 1/U_1$  [17], and  $\epsilon$  a detection efficiency of 0.68.  $U_0$  is a flow rate into the guide,  $U_0 = 1/4v_{av}S$ , where  $v_{av}$  is the average UCN velocity of 3.1 m/s at the valve and  $S$  the guide-tube cross section.  $U_{90}$  is a  $90^\circ$  bend conductance and  $U_1$  the conductance of the vertical guide including the hole, which are represented by the products of  $U_0$  and transmission probabilities  $C_{90}$  and  $S_{\text{hole}}/S = (1/8.5)^2$ , respectively.  $S_{\text{hole}}$  is the hole area.  $C_{90}$  was estimated to be  $1/2$ . Thus,  $U \cong U_1$ .

We have increased the proton irradiation time up to 600 s. The measured UCN counts as a function of time for a proton current of  $1 \mu\text{A}$  are shown in Fig. 4(a). From this measurement, a UCN density of  $15 \text{ UCN cm}^{-3}$  at  $E_c = 90$  neV was obtained. UCNs of energies from 125 to 210 neV at production contribute to filling the horizontal guide tube. Here, the energies are measured at the bottom of the He-II bottle. The UCN density does not reach the full value of statistical equilibrium, but 80%, because the estimated filling time of 12 s is rather long. The number of UCNs in the horizontal and vertical tubes was estimated by means of the density and effective volumes including the enlargement of the momentum space at lower height. UCNs of energies lower than 125 neV at the bottom are confined in the vertical tubes. Including these UCNs, the total UCN number of  $1.4 \times 10^6$  was deduced. From this, a UCN density of  $180 \text{ UCN cm}^{-3}$ , produced in the 8 L He-II, is obtained, and, finally, the UCN production rate in the He-II was determined to be  $4 \text{ UCN cm}^{-3} \text{ s}^{-1}$  at  $E_c = 210$  neV with  $\tau_s = 47$  s.

A  $^3\text{He}$  concentration of  $10^{-12}$  in the  $^4\text{He}$  obtained by the heat-flush method [18] induces a very small loss rate:  $\tau_{^3\text{He}}^{-1} = 2 \times 10^{-5} \text{ s}^{-1}$ . The storage lifetime is limited by the wall losses. We have decreased these losses by means of alkali cleaning and baking at a temperature of  $140^\circ\text{C}$ . A storage lifetime of  $\tau_s = 81$  s was obtained as shown in Fig. 5, where the proton irradiation time was 40 s and the aperture disk was removed. The sum of UCN counts after valve opening is plotted as a function of  $t_d$ . The slightly enhanced UCN counts at  $t_d = 0$  and 20 s may arise from UCNs of marginal energies, escaping from the UCN bottle in a short time period. The sum of UCN counts for  $t_d = 0$  becomes 280 000 for a proton irradiation of 240 s. The UCN density at the UCN valve becomes  $26 \text{ UCN cm}^{-3}$ .

*Cryogenic test.*—We have measured He-II and  $^3\text{He}$  temperatures by using LakeShore cerox thermometers in the double tube and the liquid  $^3\text{He}$  vessel. The heat load on the liquid  $^3\text{He}$  was measured by a KOFLOC mass-flow meter in the  $^3\text{He}$  gas circulation line. The results are shown in Fig. 4(b). The He-II temperature gradually increased from 0.77 to 0.83 K during the proton-beam bombardment with a

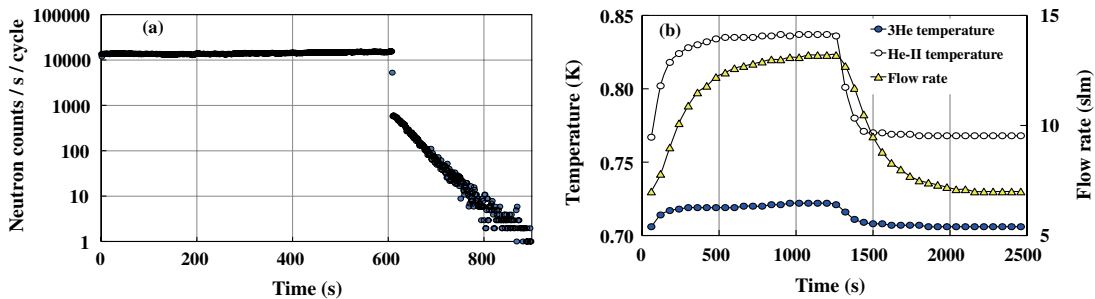


FIG. 4 (color online). (a) UCN production with a proton-beam current of  $1 \mu\text{A}$  and a duration of 600 s. The closed circles are neutron counts with the annular disk in front of the detector. (The start of UCN count was delayed by 2 s after switching off the proton beam.) (b) Effect of a 1200 s proton-beam impingement on the He-II system. The open and closed circles are He-II temperatures and  $^3\text{He}$  temperatures, respectively. The triangles are  $^3\text{He}$  gas flows in the  $^3\text{He}$  circulation line.

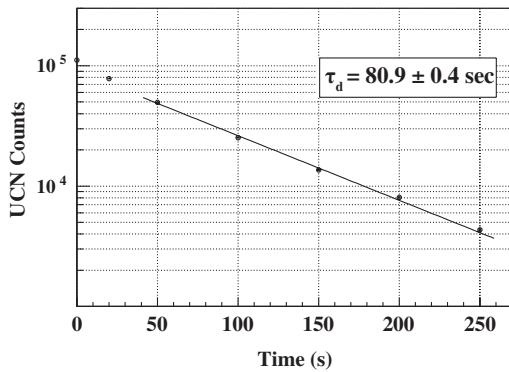


FIG. 5. Storage lifetime after alkali cleaning and high temperature baking. The UCN counts for 0, 25, 50, 100, 150, 200, and 250 s delay times of UCN valve opening after the beam was stopped are shown.

power of  $400 \text{ MeV} \times 1 \mu\text{A}$ . After switching off the beam, the temperature returned slowly to 0.77 K. These gradual changes are caused by the finite value of the heat capacity, which increases the time constant. Similarly, the  $^3\text{He}$  gas circulation rate also changes gradually. This means that the heat load in the He-II causes not only the temperature rise in the He-II itself but also the evaporation of the liquid  $^3\text{He}$ . This result shows that a large volume of He-II will buffer the  $\gamma$  heating during proton-beam bombardment at higher currents. We have also simulated the  $\gamma$  heating by using a heater, wound around the He-II bottle. We found similar variations in the He-II and  $^3\text{He}$  temperatures and the  $^3\text{He}$  flow rate when a heater power of 160 mW was applied. This rather high heat load compared with the Monte Carlo calculation may be a result of  $\beta$  radiation heating in the He-II bottle, which is not included in PHITS code.

The result of the cryogenic test shows that the present UCN source can provide  $P = 40 \text{ UCN cm}^{-3} \text{ s}^{-1}$  at  $E_c = 210 \text{ neV}$  and  $\tau_s = 81 \text{ s}$  with an acceptable He-II temperature rise when a 5 times higher speed of  $^3\text{He}$  pumping is used, which is commercially available. Also a 5 times larger heat exchanger between  $^4\text{He}$  and  $^3\text{He}$  is required. The UCN density at  $E_c = 90 \text{ neV}$  in the horizontal guide is expected to be  $260 \text{ UCN cm}^{-3}$ . The necessary proton-beam power for the production of spallation neutrons is

readily available at several laboratories. Thus, we expect the present UCN source to be a very useful facility for conducting UCN experiments.

We express our thanks to A. Suzuki and H. Toki for their warm encouragements and to G. P. A. Berg for his critical reading of the manuscript. This work is supported by Grants-in-Aid for Scientific Research No. 21224007.

- 
- [1] M. Cohen and R. Feynman, *Phys. Rev.* **107**, 13 (1957).
  - [2] L. Landau, *J. Phys. USSR* **11**, 91 (1947).
  - [3] R. Golub and J. Pendlebury, *Phys. Lett. A* **62**, 337 (1977).
  - [4] R. Golub, C. Jewell, P. Ageron, W. Mampe, B. Heckel, and I. Kilvington, *Z. Phys. B* **51**, 187 (1983).
  - [5] H. Yoshiki, K. Sakai, M. Ogura, T. Kawai, Y. Masuda, T. Nakajima, T. Takayama, S. Tanaka, and A. Yamaguchi, *Phys. Rev. Lett.* **68**, 1323 (1992).
  - [6] P. Huffman *et al.*, *Nature (London)* **403**, 62 (2000).
  - [7] C. Baker *et al.*, *Phys. Lett. A* **308**, 67 (2003).
  - [8] O. Zimmer, K. Baumann, M. Fertl, B. Franke, S. Mironov, C. Plonka, D. Rich, P. Schmidt-Wellenburg, H. F. Wirth, and B. vandenBrandt, *Phys. Rev. Lett.* **99**, 104801 (2007).
  - [9] E. Korobkina, R. Golub, B. Wehring, and A. Young, *Phys. Lett. A* **301**, 462 (2002).
  - [10] C. Morris *et al.*, *Phys. Rev. Lett.* **89**, 272501 (2002).
  - [11] F. Atchison *et al.*, *Phys. Rev. Lett.* **95**, 182502 (2005).
  - [12] Y. Masuda, T. Kitagaki, K. Hatanaka, M. Higuchi, S. Ishimoto, Y. Kiyonagi, K. Morimoto, S. Muto, and M. Yoshimura, *Phys. Rev. Lett.* **89**, 284801 (2002).
  - [13] K. Niita, N. Matsuda, Y. Iwamoto, H. Iwase, T. Sato, H. Nakashima, Y. Sakamoto, and L. Sihver, JAEA Technical Report JAEA-Data/Code No. 2010-022, 2010.
  - [14] K. Inoue, *J. Nucl. Sci. Technol.* **7**, 580 (1970).
  - [15] Y. Masuda, S. Ishimoto, M. Ishida, Y. Ishikawa, M. Kohgi, and A. Masaike, *Nucl. Instrum. Methods Phys. Res., Sect. A* **264**, 169 (1988).
  - [16] F. Atchison, T. Brys, M. Daum, P. Fierlinger, A. Formin, R. Henneck, K. Kirch, M. Kuzniak, and A. Pichlmaier, *Nucl. Instrum. Methods Phys. Res., Sect. A* **552**, 513 (2005).
  - [17] R. Golub, D. Richardson, and S. Lamoreaux, *Ultra-Cold Neutrons* (Hilger, London, 1991).
  - [18] P. McClintock, *Cryogenics* **18**, 201 (1978).